Prof. MARÍA BLANCA ROS LATIENDA, Professor of the Organic Chemistry Department of the Faculty of Sciences of the University of Zaragoza

and

Dr. TERESA SIERRA TRAVIESO, Research Scientist of the Spanish Council for Scientific Research (CSIC) of the Aragon Materials Science Institute (ICMA) of the University of Zaragoza-CSIC

PLACE ON RECORD:

That the Report "Nanostructured systems for drug delivery" has been carried out under their supervision by MARTÍN CASTILLO VALLÉS in the Organic Chemistry Department of the University of Zaragoza.

Prof. María Blanca Ros Latienda Dr. Teresa Sierra Travieso

Acronyms

bis-MPA	2,2-*bis*(hydroxymethyl)propionic acid
CLPMs	Cross-Linked Polymeric Micelles
CMC	Critical Micelle Concentration
CPT	Camptothecin
CQ	Chloroquine
DLS	Dynamic Light Scattering
DMSO	Dimethyl sulfoxide
DNA	Deoxyribonucleic acid
FT-IR	Fourier Transform Infrared Spectroscopy
HCV	Hepatitis C Virus
NMR	Nuclear Magnetic Resonance
PEO	Polyethylene oxide
PPO	Polypropylene oxide
PVDF	Polyvinylidene fluoride
SEM	Scanning Electron Microscopy
TEM	Transmission Electron Microscopy

Index

1. INTRODUCTION

Drug delivery refers to approaches for transporting drugs in the body, with the objective to achieve **site-targeting in the organism**. Drug delivery technologies modify drug release profile, absorption, distribution and elimination, giving rise to an **improvement in drug efficacy and safety** over the free form of the bioactive agent. An ideally controlled release of a drug means that the liberation of the pharmacological compound is produced in a constant and prolonged way, not exceeding the toxicity levels but surpassing the minimum effective level.

In order to achieve a controlled release of drugs, the use of **nanocarriers** in drug delivery has been proposed[1]. These systems can provide many advantages, such as the **improvement of drug solubility and stability** in the bloodstream, the **reduction of drug toxicity** and its associated side effects thanks to the reduction of the doses, the **increasing of immune responses** in vaccine formulations, the use of **sensitive nanocarriers** that only release the drug when external stimuli is applied, and the potential to **deliver drugs in a targetable manner**, delivering sufficiently high local amounts to avoid the development of resistant parasite strains.

One of the most important features of nanocarriers is their size, since it controls the dwell time in the bloodstream, as well as their internalization within the cell and bioavailability of drug-containing nanoparticles[2]. Nanocarriers with sizes ranging from 10 to 100 nm are optimal for the application in drug delivery.

Among the different types of nanocarriers assayed as drug delivery systems, **polymeric micelles** have been successful for biomedical applications[3],[4],[5]. Polymeric micelles are aqueous dispersions of **amphiphilic block copolymers** that form particles of nanometric size (10-1000 nm). This kind of structures presents features of both nanoparticles and hydrogels, i.e. the ability to interact with biological systems due to its small size, as well as to hold large amounts of water. Polymeric micelles can be stabilized by crosslinking providing **Cross-Linked Polymeric Micelles (CLMPs)**[6],[7], in which the preformed micellar assemblies are blocked via covalent bonding.

CLPMs must be composed of biodegradable compounds, allowing a stable and prolonged liberation of the drug as the carrier degrades. Due to the amphiphilic nature of the constituent polymer, which results in the formation of a lipophilic core and a hydrophilic shell, **CLPMs can encapsulate both liposoluble and hydrosoluble drugs**

within their polymeric matrix. Drugs can be captured by non-covalent interactions (ionic interactions, hydrogen bonding, hydrophobic interactions, etc.) or covalently incorporated within the polymeric structure.

Moreover, drug liberation can also be controlled by using **CLPMs that respond to external stimuli**[8]. This kind of materials is able to **modify its structural composition or conformation** when a certain physical or chemical stimuli is produced, promoting the controlled liberation of the active species previously encapsulated in the nanocarrier. **Thermosensitive CLPMs** are one of the most studied systems, and they are composed of polymeric materials that contain thermosensitive units in their structure[9]. These stimuli-responsive materials modify their conformation when the temperature varies, presenting an expanded conformation at low temperatures, which allows an easy entry and exit of the encapsulated drug, whereas at higher temperatures the nanocarrier contracts, holding the drug within the polymeric matrix and giving rise to a slower and more controlled drug release.

Pluronic® F-127 is an amphiphilic block copolymer widely used to form nanocarriers for drug delivery, among many other biomedical applications[10],[11]. It is composed by two polyethylene oxide (PEO) units separated by a central polypropylene oxide (PPO) unit. Moreover, **Pluronic© F127 presents thermoresponsive properties**. This compound is soluble in water at low temperatures and is able to self-arrange in water above a certain temperature (Critical Micelle Temperature) and concentration (Critical Micelle Concentration), forming micelles consisting of a hydrophobic PPO core and a hydrophilic PEO shell.

Furthermore, in the search for new materials that self-assemble in water to form nanocarriers, **hybrid linear-dendritic block copolymers** have been proposed in the last years[12]. These structures are formed by the **combination of linear chains of a polymer and dendritic segments** in the chain's end. **Dendritic structures are highly branched macromolecules** composed of three parts: the core, the branching units that give rise to the different generations, and the periphery, which allows the introduction of a wide variety of functional groups. The number of functional groups in the periphery is determined by the generation. Dendrimers based on 2,2-*bis*(hydroxymethyl)propionic acid (*bis*-MPA) present several features that make them ideal candidates for their use in biomedical applications, i.e. their *in vivo* and *in vitro* biocompatibility, their solubility in

biological environments and their ability to degrade through a hydrolytic process of the ester bonds[13].

Joining these trends and requirements, the *Liquid Crystals and Polymers* research group initiated a new working approach focused on **CLPMs** from **thermoresponsive linear-dendritic block copolymers based on Pluronic® F127** to be used as drug delivery nanocarriers[14],[15], with encouraging results opening new design possibilities which inspire the current research master project.

2. OBJECTIVES AND WORKING PLAN

The aims of this research work are the **design and synthesis of new amphiphilic block copolymers** with the ability to self-arrange in water forming micelles, **which will be photopolymerized** in order to obtain **cross-linked polymeric micelles**, with applications as **nanocarriers** in drug delivery.

The motivations and plan followed in the realization of this work consists of the steps outlined below:

1) Design, synthesis and characterization of the Pluronic® F127 derivatives:

Starting from the commercial block copolymer Pluronic® F127, two different derivatives will be synthesized (*Scheme 1)*. The first one will be a **linear block copolymer** derivative, **F127-A-2**, whereas the second compound will be a **hybrid dendritic-linear-dendritic block copolymer, F127-A-4**. They both incorporate **carbamate moieties** within their structure with the aim of promoting hydrogen bonding interactions, which could affect both the micellization process and the interaction with the encapsulated molecules, thereby increasing the load capacity of the corresponding CLPMs. In the case of the hybrid dendritic-linear-dendritic derivative, a first generation dendron of *bis*-MPA will be incorporated, in order to increase the number of functional groups in the polymer periphery. Finally, both Pluronic® F127 derivatives will be functionalized with **acrylate groups**, allowing their crosslinking by means of photopolymerization. The linear compound will present two acrylate groups in the chain's end, whereas the hybrid dendritic-linear-dendritic one has four photopolymerizable groups in the periphery.

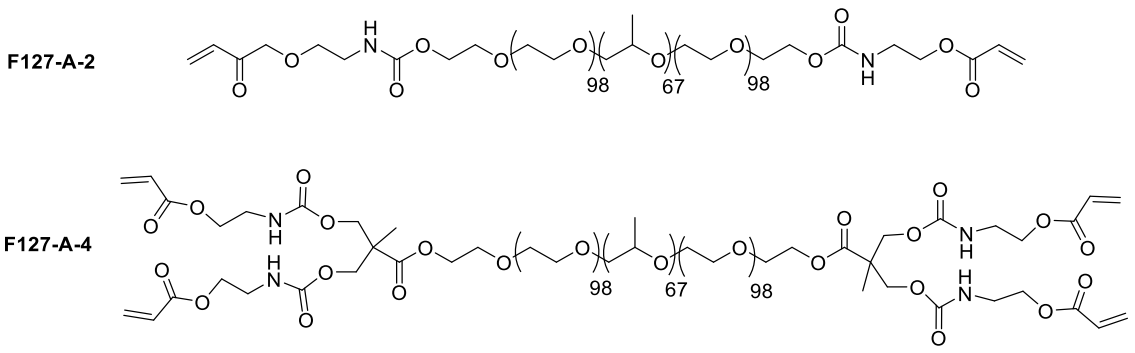

Scheme 1. Chemical structure of synthesized Pluronic® F127 derivatives.

The two synthesized compounds, as well as the intermediates of their preparation, will be chemically characterized by conventional characterization techniques, i.e. ^{1}H-NMR, ^{13}C-NMR and FT-IR.

2) Preparation of CLPMs in water

CLPMs will be obtained by means of the photopolymerization of micellar aggregates of the Pluronic® F127 derivatives formed in water. To achieve this objective, the **Critical Micelle Concentration** (CMC) will be first determined for both derivatives in order to know the exact concentration above which the block copolymers started to self-assemble. Then, polymer solutions of concentrations above the CMC will be prepared, and the structure of the preformed micelle aggregates will be fixed through photocrosslinking in presence of a commercial photoinitiator.

Photocrosslinking at different concentrations of the block copolymers will be carried out in order to determine its influence in the final shape and size of the CLPMs.

3) Morphological characterization of CLPMs

CLPMs morphology will be studied by different characterization techniques suitable for nanometric materials, i.e. **DLS, TEM and SEM**. Moreover, since CLPMs are composed by thermosensitive materials, the **temperature influence in size** will be also studied.

4) Drug encapsulation

Finally, CLPMs will be tested for their application as nanocarriers. Two different drugs, a liposoluble (**camptothecin**) and a hydrosoluble one (**chloroquine**), will be encapsulated. For this purpose, two **different encapsulation techniques** will be employed.

3. RESULTS AND DISCUSSION

3.1. Synthesis and characterization of Pluronic® F127 derivatives

3.1.1. Synthesis and characterization of the linear Pluronic® F127 derivative, **F127-A-2**.

The synthetic route followed to obtain **F127-A-2** consists of several steps detailed in *Scheme 2*.

Firstly, commercial Pluronic© F-127 was made to react with *p*-nitrophenyl chloroformate, giving rise to **F127-NP-2**. The *p*-nitro phenyloxy group of the obtained carbonate functionality acted as a good leaving group, and in presence of ethanolamine reacted with its amino group to form a carbamate, resulting in **F127-C-2**. Finally, acrylate groups were introduced by means of the reaction of the hydroxyl groups in **F127-C-2** with acryloyl chloride. In the first attempts, the full functionalization of **F127-C-2** with acrylate groups was not achieved.

In order to completely incorporate the acrylate groups, different reaction conditions were checked. The presence of a little amount of water entrapped within the polymer and in the reaction solvent was proved to be one of the problems that caused the incomplete functionalization, since it quickly reacts with acryloyl chloride to give rise to the non-reactive carboxylic acid. Therefore, first, freshly distilled dichloromethane was used as the reaction solvent, and **F127-C-2** was thoroughly dried under vacuum and above its boiling point. Secondly, the concentration of reactants was also a key point. Finally, the complete functionalization was achieved for dry conditions and using the smallest amount of solvent to solubilize the reagents during the reaction.

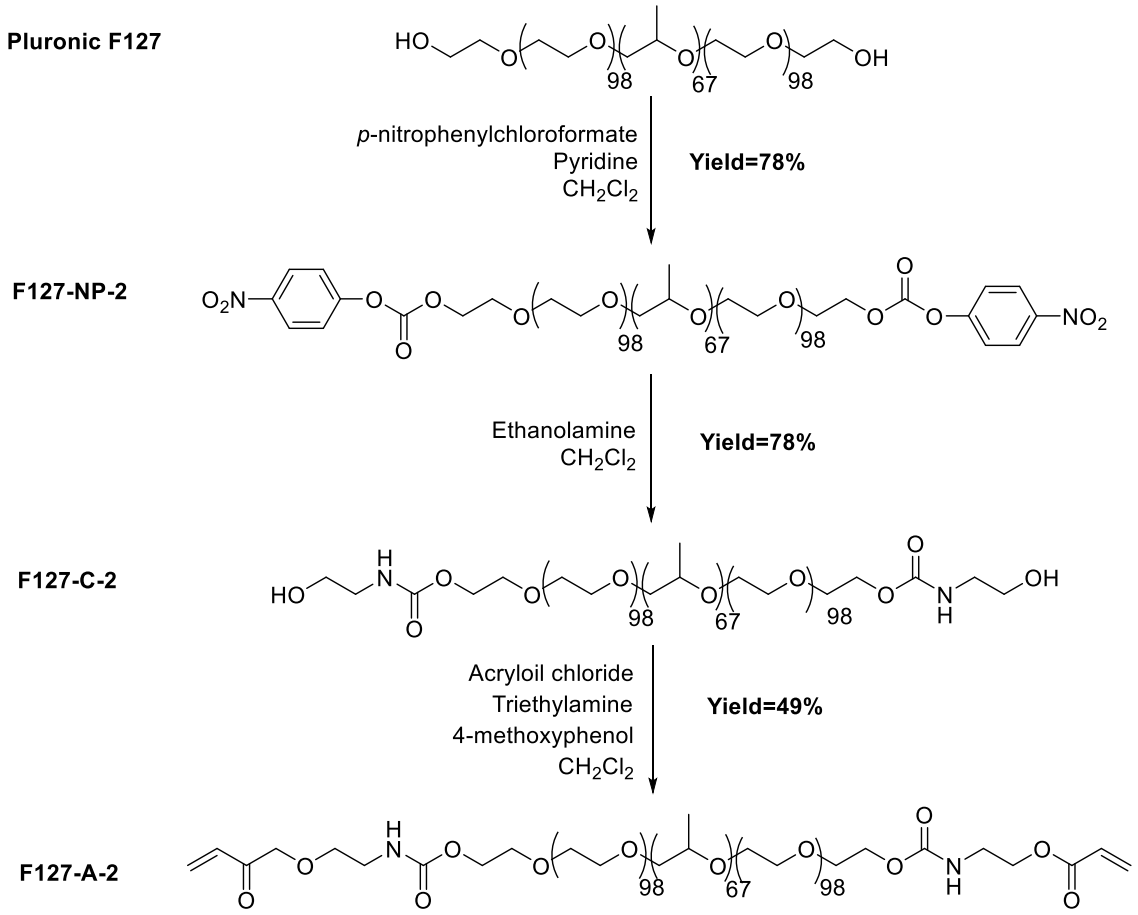

*Scheme 2. Synthetic route to obtain **F127-A-2**.*

The correct functionalization of Pluronic© F-127 in each step of the synthetic route was corroborated by NMR and FT-IR.

Pluronic© F-127 present two characteristic signals in the ^{1}H-NMR spectrum. The first one appears at 1.12 ppm and integrates for 201 H corresponding to the methyl groups in the PPO block. The second one emerges as a complex signal from 3.30 to 3.70 ppm and integrates for about 1100 H, corresponding to the hydrogen atoms corresponding to the H-C-O systems in both PPO and PEO blocks. When Pluronic© F-127 is functionalized, the presence of new signals, and specially their relative integration in comparison with the Pluronic signals, provides useful information to discern whether the functionalization was successfully achieved or not.

In the case of **F127-NP-2** (*Figure 1)*, three new signals appear in the ^{1}H-NMR spectrum with respect to Pluronic© F-127. A multiplet integrating for 4 H at 4.41 ppm, which corresponds to PPO block protons directly linked to the carbonate group, is observed, since these hydrogen atoms are no more similar to those of the rest of the PPO chain. In

addition, two signals, integrating for 4 H each one, appear at 7.39 ppm and 8.27 ppm. These signals correspond to the hydrogen atoms of the aromatic ring.

The correct synthesis of **F127-C-2** can be checked by the displacement of the multiplet from 4.41 ppm to 4.21 ppm (*Figure 1*), due to the transformation of the carbonate group to a carbamate one, as well as by the disappearance of the two signals at 7.39 ppm and 8.27 ppm corresponding to the aromatic protons. In addition, a broad signal appears at 5.51 ppm. This signal corresponds to the N-H protons of the carbamate group.

Finally, the ^{1}H-NMR spectrum of **F127-A-2** (*Figure 1*) shows three new doublets of doublets integrating for 2 H each one between 5.84 ppm and 6.44 ppm. These signals are characteristic of acrylate groups, and their correct integration confirms the complete functionalization.

Pluronic© F-127 derivatives were also characterized by means of ^{13}C-RMN. However, some of the characteristic peaks corresponding to the functionalization of the ends of the chain were difficult to observe. Specially, the signal corresponding to the carbonyl carbon atoms was very weak and difficult to assign.

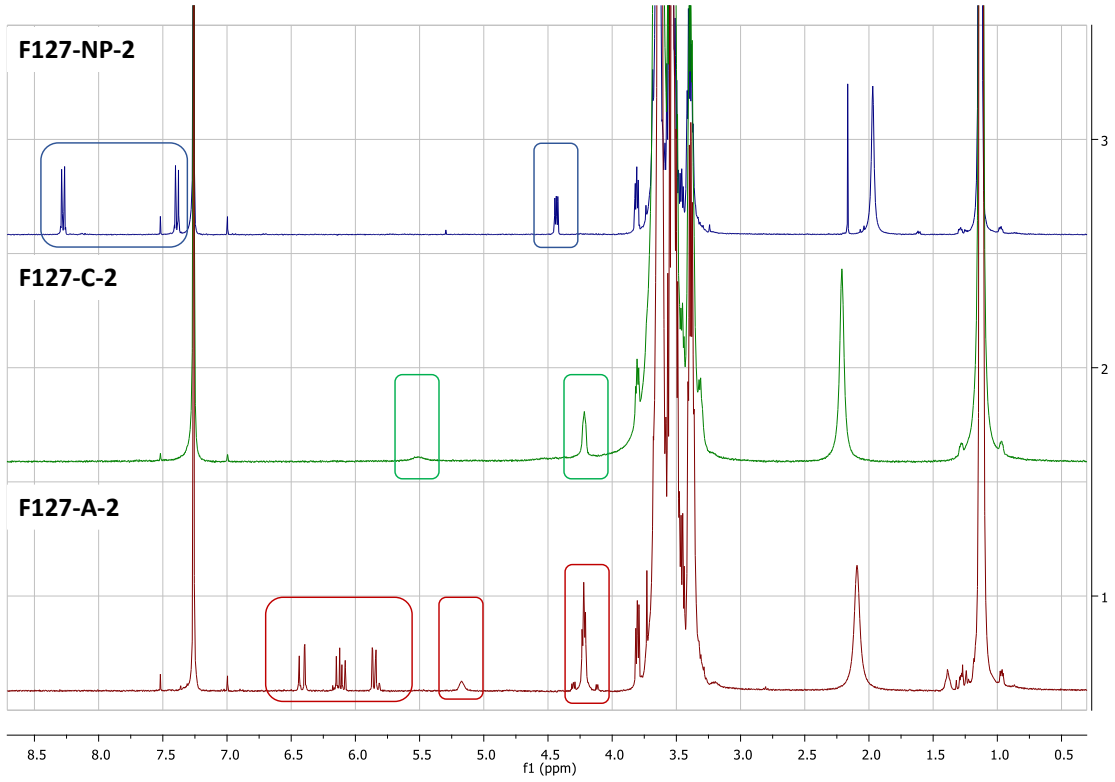

*Figure 1. ^{1}H-NMR spectra of **F127-NP-2**, **F127-C-2** and **F127-A-2** in $CDCl_3$ (400 MHz).The assignment of each signal is detailed in the Annexes.*

In addition to NMR, FT-IR has been used to follow the reactions. The FT-IR spectra of **F127-NP-2**, **F127-C-2** and **F127-A-2** are shown in *Figure 2*. The peak corresponding to the stretching vibration of the C=O bond provides useful information to determine if the carbonate group of **F127-NP-2** has been replaced by a carbamate group in **F127-C-2** and **F127-A-2**. In **F127-NP-2**, this peak appears at 1765 cm^{-1}, whereas in **F127-C-2** and **F127-A-2**, the peaks are shifted to lower wavenumbers: 1722 cm^{-1} and 1728 cm^{-1} respectively. Moreover, the presence of hydroxyl groups at both ends of the chain can also be observed in the FT-IR spectrum. Pluronic© F-127 and **F127-C-2** present hydroxyl-terminated chains. Thus, a wide signal is observed from 3500 to 3200 cm^{-1}. These signals, which correspond to the stretching of the O-H bond in hydroxyl groups, are not observed in the spectra of **F127-NP-2** and **F127-A-2**.

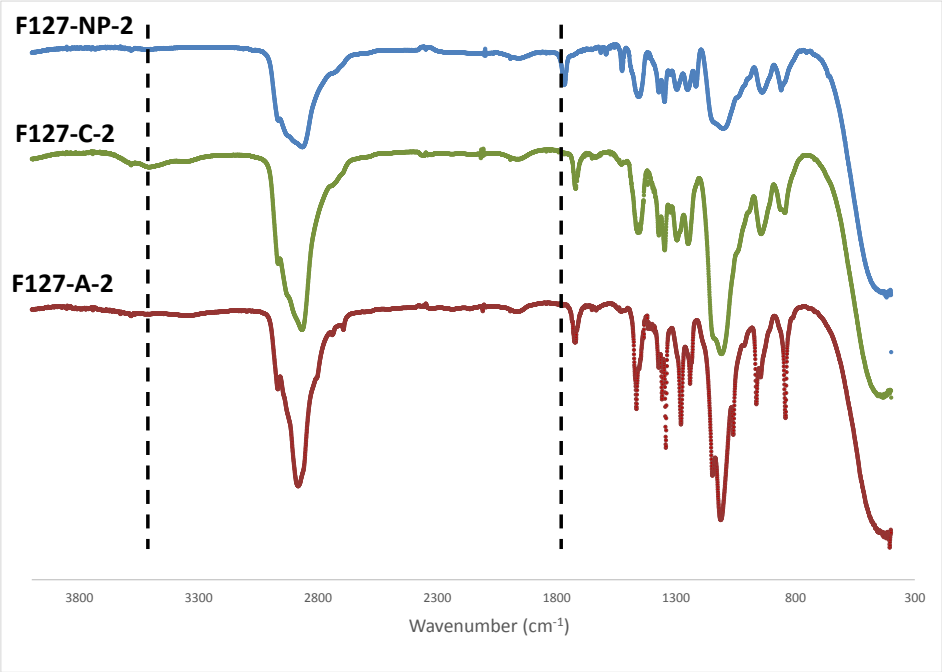

*Figure 2. IR spectra of **F127-NP-2**, **F127-C-2** and **F127-A-2** (neat on NaCl). Presence and absence of the O-H stretching band and displacement of the stretching C=O vibration for each compound.*

3.1.2. Synthesis and characterization of the hybrid dendritic-linear-dendritic Pluronic® F127 derivative, **F127-A-4**.

The synthetic route followed to obtain **F127-A-4** consists of several steps detailed in *Scheme 3*.

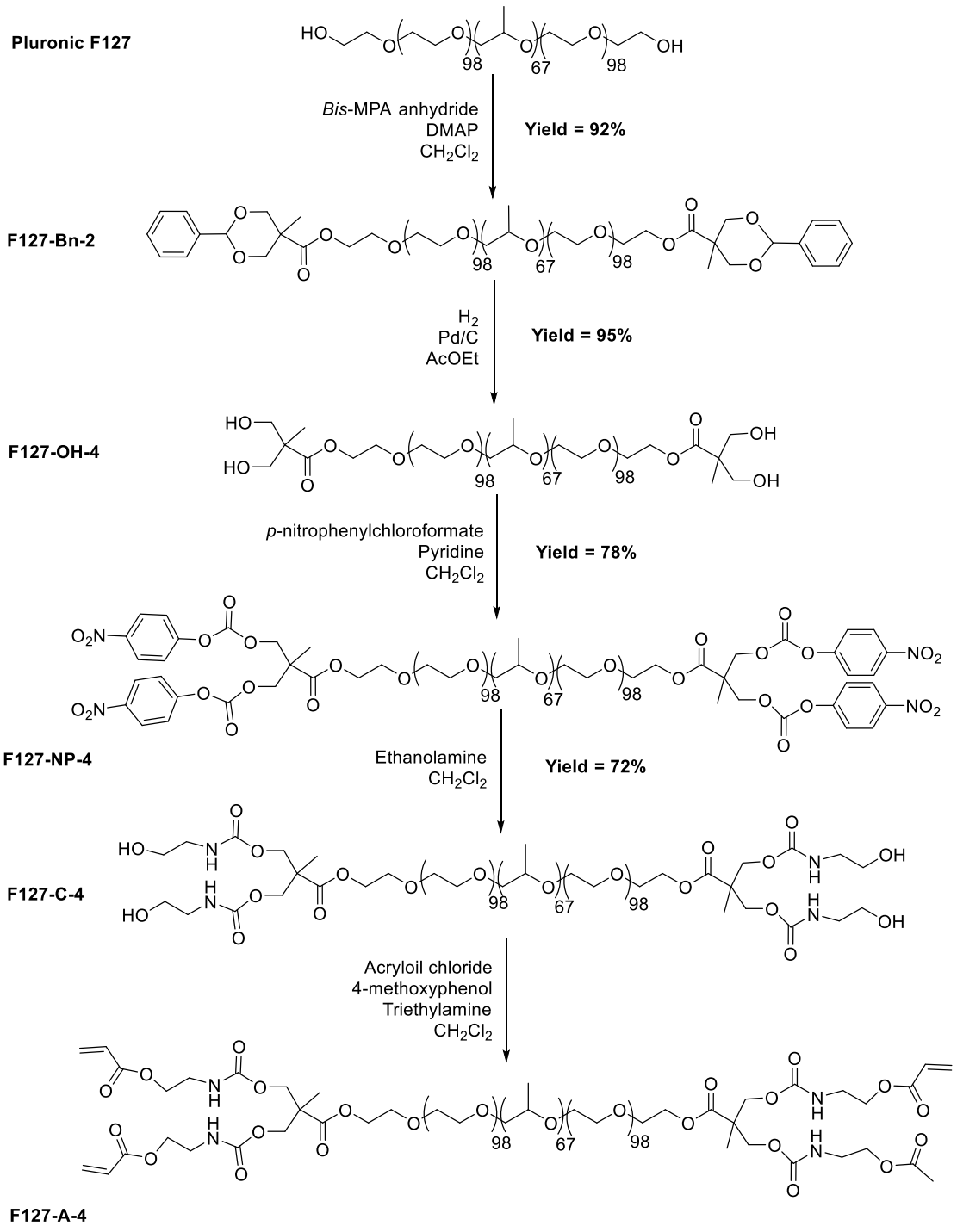

*Scheme 3. Synthetic route to obtain **F127-A-4**.*

Starting from commercial Pluronic© F-127, the reaction with benzylidene-2,2-*bis*(oxymethyl) propionic anhydride gave rise to **F127-Bn-2**[16]. This anhydride was previously synthesized from commercial 2,2-*bis*(hydroxymethyl) propionic acid, which was first made react with benzaldehyde dimethyl acetal to protect the hydroxyl groups and subsequently condensed to obtain the respective anhydride. The hydroxyl groups of **F127-Bn-2** were deprotected by means of hydrogenation with H_2 catalyzed by Pd/C to obtain **F127-OH-4**.

The incorporation of the *bis*-MPA dendritic structure at the end of the polymeric chains increased the number of terminal hydroxyl groups from two to four. Then, the same synthetic route as in the case of the linear derivative was followed: the reaction of **F127-OH-4** with *p*-nitrophenyl chloroformate gave rise to **F127-NP-4**. The carbamate group of **F127-C-4** was obtained through reaction of **F127-NP-4** with ethanolamine. In both reactions, the conditions were adjusted in order to incorporate the four functional groups. Finally, the introduction of acrylate groups was attempted.

Unlike in the case of the linear derivative, the complete functionalization was not achieved for the hybrid dendritic-linear-dendritic Pluronic© F-127 derivative. The reaction conditions optimized for the linear derivative were applied to obtain **F127-A-4**. In addition, both trimethylamine and acryloyl chloride, the reactants used during the acrylation process, were distilled too. Moreover, the reaction time was increased up to three days. Nevertheless, only partial acrylation was accomplished, even under dry conditions, at high reactant concentrations and long reaction times. The number of acrylate groups introduced during the reaction was not reproducible. At best, a functionalization of the 60 % was achieved, as determined by the integration of the characteristic signals of acrylate groups in the ^{1}H-NMR spectrum (see Annexes). As a consequence of these results, only **F127-A-2** has been used for posterior studies of this master project.

The characterization of all the compounds obtained during the synthetic process was similar to that of the linear derivative. ^{1}H-NMR and FT-IR were used to confirm the presence of the functional groups in each step of the synthesis (see Annexes).

3.2. Preparation of CLPMs

3.2.1. Critical Micelle Concentration determination.

The Critical Micelle Concentration is a characteristic value of amphiphilic materials that defines the concentration above which they start to self-assemble forming micelles in a solvent. When **F127-A-2** is placed in water, the lipophilic chains interact with themselves to form the core and the hydrophilic parts are extended towards the aqueous solution. The lipophilic core is formed by the PPO block, whereas the hydrophilic chains are the PEO blocks. The determination of the CMC in water was required since the posterior photopolymerization process were performed at concentrations above this value, ensuring the formation of the aggregates.

For the determination of the CMC in water, the pyrene method[17] was carried out. This method is based on the difference in the excitation spectrum of pyrene depending on whether it is in a hydrophilic environment ($\lambda_{exc\ máx}$=332 nm) or in a lipophilic environment ($\lambda_{exc\ máx}$=335 nm). Therefore, in copolymer water solutions below the CMC, pyrene will be in a hydrophilic environment, whereas for copolymer concentrations above the CMC, pyrene, which is a lipophilic molecule, will be encapsulated within the lipophilic core of the self-assembled micelles. Accordingly, the encapsulation of pyrene shifts its excitation maximum from 332 nm to 335 nm. Representing the intensities ratio -I_{335}/I_{332}- versus the polymer concentration logarithm (logC), the CMC can be determined by calculating the intersection between the two linear domains of the graph (*Figure 3*).

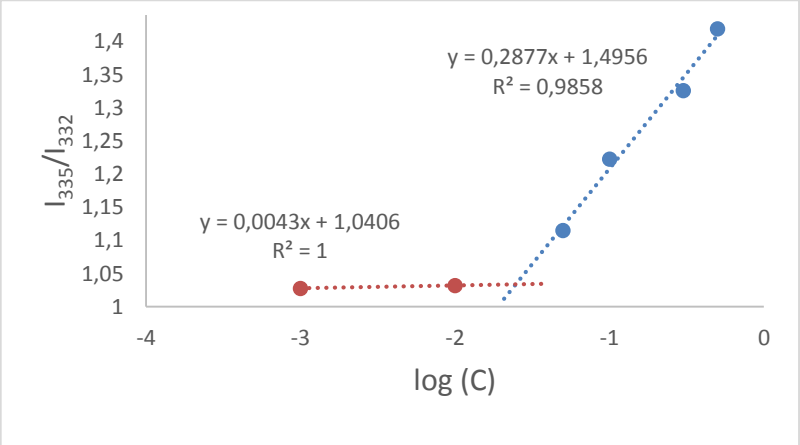

*Figure 3. Plot of the excitation maxima intensities ratio of pyerene vs **F127-A-2** concentration for CMC calculation.*

To obtain this graph, solutions of **F127-A-2** of concentrations 0.0001, 0.001, 0.01, 0.05, 0.1, 0.3, 0.5 and 1 % (w/v) were prepared (1 % (w/v) is equal to 10 mg/mL). A pyrene solution was added to obtain a final pyrene concentration of $6 \cdot 10^{-8}$ M, and the excitation spectra from 300 to 350 nm and λ_{em}=390 nm was recorded. Temperature strongly affects the CMC value, so the sample's preparation and the measurements were carried out at 25^0C.

The **CMC** for **F127-A-2** was **0.025 % (w/v)**. This value is much lower than that of Pluronic© F-127, which has a CMC of 0.25 % (w/v). The decrease in one order of magnitude of the CMC value for **F127-A-2** with respect to commercial Pluronic may be due to the effect of the presence of carbamate groups in the chain's end that favors the formation of hydrogen bonding interactions. These interactions can make the micelles more stable, decreasing the minimum concentration above which the block copolymer starts to self-aggregate.

3.2.2. Photopolymerization of self-assembled micelles.

CLPMs were prepared by means of UV photopolymerization of the reactive acrylate groups in distilled water solution containing the block copolymer **F127-A-2** and the commercial photoinitiator Irgacure 2959. After polymerization, these micelles in solution provided crosslinked nanoparticles that contain lipophilic and hydrophilic domains.

In order to study the relationship between the copolymer concentration on the size and on the load capacity of the obtained crosslinked nanoparticles, solutions of 1.4% (w/v), 0.77% (w/v) and 0.50% (w/v) of the copolymer were used to perform the photopolymerization process. All these concentrations are above the CMC, so that they ensure the self-assembly forming micelles that are necessary for the subsequent formation of the crosslinked nanoparticles. Hereinafter, photopolymerized CLPMs at the different concentrations will be named as **F127-A-2-05**, **F127-A-2-077** and **F127-A-2-140**.

The photopolymerization process was performed by irradiating the corresponding solution with UV light (λ=365 nm) at 25^0C (The photopolymerization system is depicted in the Annexes). Then, the solutions were dialyzed (MWCO 300,000 membrane) at 4^0C in order to disaggregate the non-photopolymerized micelles and

remove them as the free monomer. In addition, aggregates of sizes smaller than 30 nm were removed too. Finally, the solutions were filtered through a 0.2 µm filter to eliminate the aggregates of sizes bigger than 200 nm.

After the photopolymerization, the yield of the process, as well as the final concentration of **F127-A-2-05**, **F127-A-2-077** and **F127-A-2-140** samples were determined by lyophilizing a small aliquot. The yield of the photopolymerization was 33.7%, 34.5% and 32.7% respectively. The final concentration was 1.87 mg/mL, 2.33 mg/mL and 4.20 mg/mL, respectively.

3.3. Morphological characterization of the CLPMs

3.3.1. Dynamic Light Scattering.

In order to determine the particle size of the CLPMs, DLS experiments were performed. These measurements were made at two temperatures in order to observe whether **F127-A-2-077** and **F127-A-2-140** presented thermoresponsive properties. The experimental data is detailed in *Table 1*.

*Table 1. Average size and size range of **F127-A-2** photopolymerized at different concentrations.*

Sample	***Average Size (nm)*** *(25°C)*	***Size Range (nm)*** *(25°C)*	***Average Size (nm)*** *(37°C)*	***Size Range (nm)*** *(37°C)*
F127-A-2-05	328.7	24.3-712.4	277.5	18.17-615.1
F127-A-2-077	128.5	24.4-255.0	105.0	21.04-220.2
F127-A-2-140	160.1	37.8-295.3	149.0	18.17-255.0

Regarding the results, several conclusions can be drawn. Firstly, micelles from the lowest concentration, **F127-A-2-05**, presented a much larger average size than **F127-A-2-077** and **F127-A-2-140**, and, surprisingly, also particles of sizes up to 700 nm. In fact, these sizes do not correspond to those expected for this sample because they were filtered through a 0,2 µm filter before the characterization by DLS. Thus, particles higher than 200 nm should not be observed. The explanation to this phenomenon may be that **F127-A-2-05** samples did not form highly crosslinked aggregates, due to the low concentration of the reactive polymer. Therefore, aggregates were present in a dynamic equilibrium, so that the particles can be disaggregated to pass through the filter and then

form again the bigger aggregates observed by DLS. On the other hand, **F127-A-2-077 (128 nm)** and **F127-A-2-140 (160 nm)** do not present that high particle sizes, confirming that the photopolymerization process was successfully accomplished and bigger aggregates were removed by means of filtration through the 0.2 µm filter. Accordingly, only **F127-A-2-077** and **F127-A-2-140** samples were used for further studies.

Secondly, an increase of the average size was observed when increasing the concentration of the polymer during the photopolymerization process from 0.77 % (w/v) to 1.40 % (w/v).

In addition, both types of CLPMs presented a **contraction** of their volume when the temperature was increased to 37°C for **F127-A-2-077 (105 nm)** and **F127-A-2-140 (149 nm)**. The size decrease was higher for **F127-A-2-12-077** than for **F127-A-2-140**. One reason for this effect may be that the higher amount of polymer in **F127-A-2-140** favors more compact structures during photopolymerization, and the obtained CLPMs are less susceptible of undergoing shrinkage when increasing the temperature.

3.3.2. Scanning Electron Microscopy and Transmission Electron Microscopy

In order to analyze the morphology and size of **F127-A-2-077** and **F127-A-2-140** CLPMs, SEM and TEM experiments were carried out.

In both cases, SEM images (*Figures 4a and 4b*) showed **spherical and ovoid nanoparticles** ranging from 35 to 130 nm. Particles of every size within this range were observed, although 70 to 110 nm were the predominant sizes. This wide size distribution corresponds to that observed in DLS experiments. The smaller sizes observed by this technique in comparison with those obtained by DLS can be explained because in the latter, the device detects the hydrodynamic radius of the particles, which includes the molecules of water surrounding the polymeric aggregate. In addition, the intensity method magnifies the signal corresponding to the biggest particles, and this effect may distort the average size of the population. Besides, SEM images were acquired under high vacuum conditions, and during the evacuation of the SEM chamber water molecules entrapped within the hydrophilic shell of the CLPMs were evaporated, causing a contraction that may decrease the observed size of the nanoparticles.

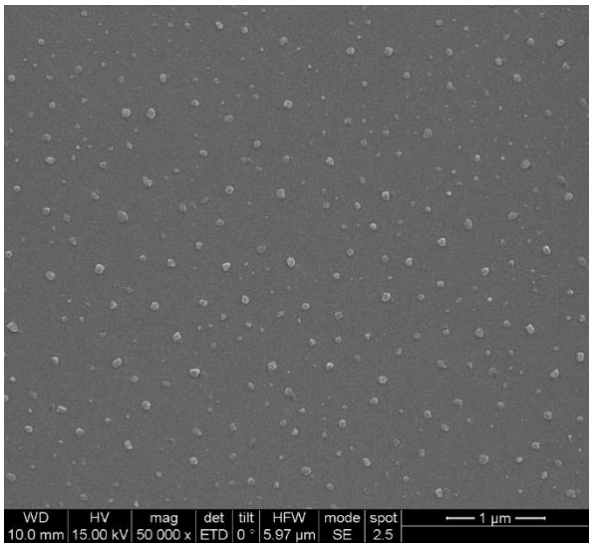

*Figure 4a. SEM image of **F127-A-2-12-077** CLPMs.*

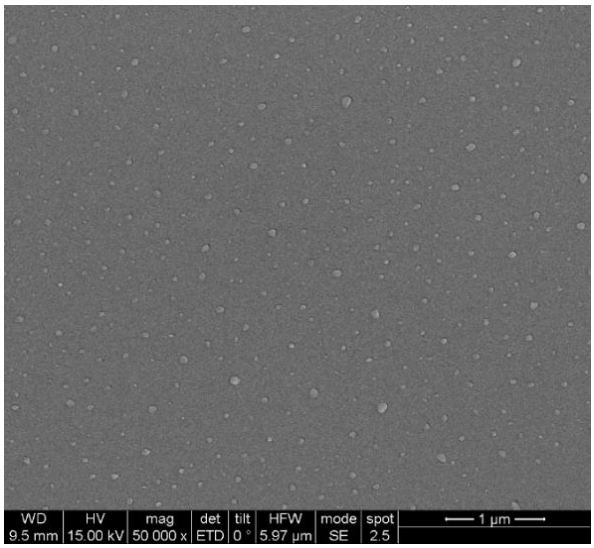

*Figure 4b. SEM image of **F127-A-2-140** CLPMs.*

TEM images (*Figures 5a and 5b*) showed spherical nanoparticles ranging from 22 to 150 nm for **F127-A-2-077** and from 26 to 141 nm for **F127-A-2-140**. These results are very similar to those observed in SEM experiments. Sizes observed by TEM were also smaller than DLS sizes, since this type of experiments are carried out at ultra-high vacuum too, evaporating the water surrounding the polymeric nanoparticles and producing the contraction of the hydrophilic shell before the acquisition of the images.

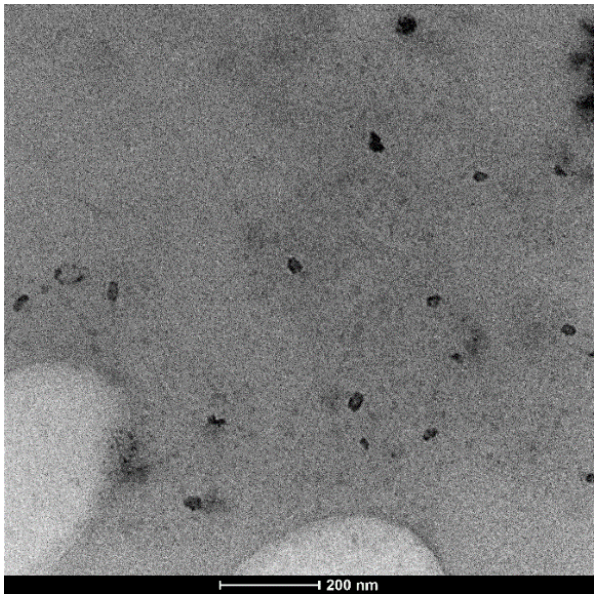

*Figure 5a. TEM image of **F127-A-2-077** CLPMs.*

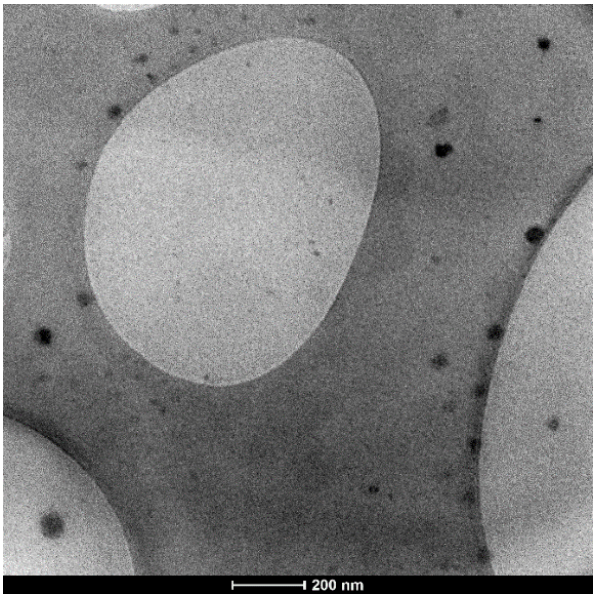

*Figure 5b. TEM image of **F127-A-2-140** CLPMs.*

3.4. Drug encapsulation experiments

In order to study the properties of the CLPMs as nanocarriers for drug delivery applications, two different compounds were encapsulated: Camptothecin (CPT), a liposoluble drug, and Chloroquine (CQ), a hydrosoluble one. The chemical structure of both drugs is depicted in *Figures 6a and 6b*.

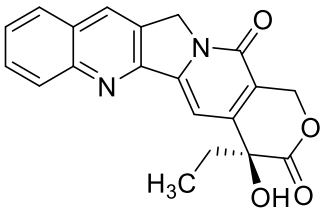

Figure 6a. Chemical structure of CPT.

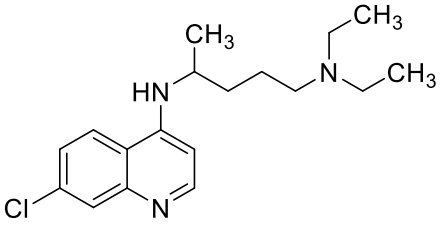

Figure 6b. Chemical structure of CQ.

3.4.1. Encapsulation of Camptothecin.

Camptothecin is a poorly water-soluble drug that exhibits remarkable activity against different types of cancer[18]. In addition, it has been recently described as a potent antiviral agent for HCV[19]. However, CPT presents some drawbacks that limit its application in medicine, i.e. very low water solubility and chemical instability due to hydrolysis of its lactone ring under physiological conditions.

F127-A-2-077 and **F127-A-2-140** CLPMs were tested as nanocarriers for the encapsulation of CPT. The **solvent diffusion method**[20] was used in order to encapsulate CPT. Commercial CPT was dissolved in DMSO and added to a 1mg/mL solution of CLPMs in distilled water. The mixtures were mechanically stirred at room temperature to ensure the correct encapsulation of CPT within the CLPMs. Then, the mixtures were dialyzed against water in order to remove the DMSO, causing precipitation of non-encapsulated CPT. The samples were filtered through a 0.45 µm PVDF filter, removing non-encapsulated CPT. Two aliquots were lyophilized, redissolved in DMSO and encapsulated CPT was quantified by fluorescence emission spectrum (λ_{max}=436 nm in DMSO, λ_{exc}=368 nm). The fluorescence calibration curve is depicted in the Annexes. The load capacities and encapsulation efficiencies are detailed in *Table 2*. As it can be seen, load capacity of **F127-A-2-077** and **F127-A-2-140** CLPMs was very similar **(around 0.46 µg/mg)**.

*Table 2. Camptothecin load capacity and encapsulation efficiency of **F127-A-2** CLPMs.*

Sample	***Load capacity (µg CPT / mg CLPM)***	***Encapsulation efficiency (% w)***
F127-A-2-077	0.475	0.36
F127-A-2-140	0.444	0.34

Additionally, preliminary studies of drug release for these materials were performed. When loaded CLPMs were dialyzed for a week, encapsulated CPT was completely released, not observing any emission in the fluorescence spectrum.

3.4.2. Encapsulation of Chloroquine.

Chloroquine is a water-soluble drug mainly used to prevent and to treat malaria, as well as in cancer therapy[21],[22],[23].

F127-A-2-077 and **F127-A-2-140** CLPMs were tested for the encapsulation of CQ. In this case, due to the good solubility of CQ in water, **the solvent/oil water emulsion method** was employed[20]. A 0.75 mg/mL solutions of CLPMs in distilled water were extracted with dichloromethane by means of mechanical stirring. Then, commercial CQ disphosphate salt in distilled water was added to the CLPMs solution in dichloromethane, and the mixture was mechanically stirred until the organic phase was completely evaporated, causing the encapsulation. The final concentration of the CLMPs and the CQ was 0.50 mg/mL.

Solutions were dialyzed against distilled water overnight in order to remove the non-encapsulated CQ. Encapsulated CQ was indirectly quantified by measuring the UV-vis absorbance of the dialysis waters. The UV-vis calibration curve is depicted in the Annexes. The load capacities and encapsulation efficiencies are detailed in *Table 3*.

*Table 3. Chloroquine load capacity and encapsulation efficiency of **F127-A-2** CLPMs.*

Sample	***Load capacity (µg CQ / mg CLPM)***	***Encapsulation efficiency (% w)***
F127-A-2-077	135.8	23.9
F127-A-2-140	293.5	45.4

In addition, the load capacity of **F127-A-2-140** CLPMs **(293.5 µg/mg)** was more than two times higher than the load capacity of **F127-A-2-077** CLPMs. This significant

increase in the load capacity may be produced by the higher size of the **F127-A-2-140** CLPMs, since larger particles will have a larger hydrophilic shell, being able to encapsulate more drug amount.

CLPMs of F127-A-2 were proved to have a **good load capacity** for the encapsulation of hydrosoluble compounds, like **CQ**. On the other hand, liposoluble compounds, e.g. **CPT, were poorly encapsulated**. This effect may be due to the higher availability of the hydrophilic shell in comparison with the lipophilic core. Thus, the encapsulation of hydrosoluble drugs is easier since they do not have to penetrate to the core.

Moreover, it is known that Pluronic® F-127 derivatives can form hydrogels at high polymer concentrations[24]. Thus, CLPMs could behave as nanostructured hydrogels, i.e. nanogels, entrapping a large amount of water within the polymeric network. Since CQ is a hydrosoluble compound, the presence of water in the interior of the CLPMs could increase the load capacity whereas this effect will not occur for a liposoluble compound like CPT.

3.5. In-vitro anti-HCV studies

In order to study the possibility of the CLPMs to act as nanocarriers for anti-HCV drugs, cytotoxicity and anti-HCV effectiveness experiments were carried out with camptothecin encapsulated in **F127-A-2-077** CLPMs[25]. These experiments were made in collaboration with researchers from the Institute for Biocomputation and Physics of Complex Systems (BIFI).

Cytotoxicity of free CPT, encapsulated CPT and CLPMs was determined by cell metabolism assays, adding increasing amounts of free CPT, encapsulated CPT and CLPMs to HuH52 cells.

To determine the anti-HCV effectiveness of encapsulated CPT, HCV replicon inhibition was monitored. The HCV replicon incorporated a DNA fragment responsible for producing a luciferase protein. Therefore, inhibition of the HCV virus replication can be observed by means of the decrease in luminescence of the cell culture.

Experimental conditions were conditioned by the low CPT encapsulation level in the CLPMs, so that the amount of water solution containing the CLPMs which was added to the cell culture was very high, diluting culture medium. As a consequence cells did not have a sufficient amount of nourishment, decreasing the cell viability.

Cytotoxicity of free CPT and encapsulated CPT is detailed in *Figure 7* As it can be observed, encapsulated CPT presented **higher** cell viabilities **in comparison with free CPT** at low CPT concentrations, whereas cytotoxicity of both samples was almost the same at high CPT concentrations. In addition, **CLPMs** always presented **cell viabilities above 80%**.

Anti-HCV effectiveness experiments were also performed. Unfortunately, due to the high amount of encapsulated CPT-containing solution that was added to the cell culture, these experiments did not offered conclusive results. New experiments have to be carried out in order to determine whether encapsulated CPT has anti-viral effects or not.

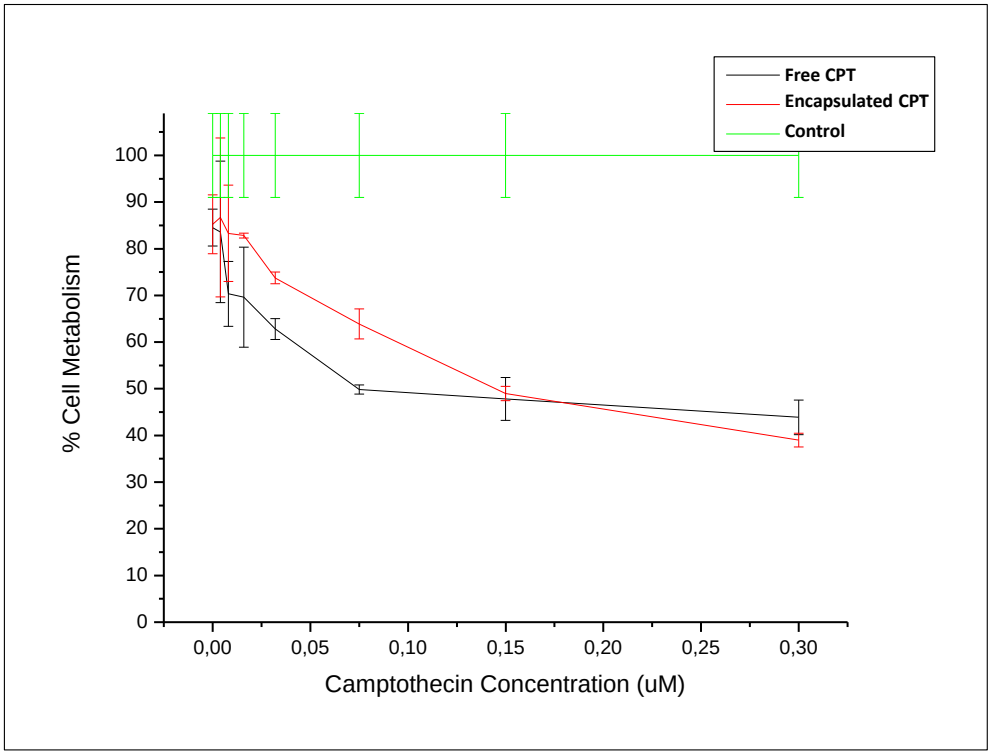

*Figure 7. Cell titter experiment for CPT and **F127-A-2-077** CLPMs.*

4. EXPERIMENTAL SECTION

4.1. Synthesis of the linear Pluronic derivative

·Synthesis of F127-NP-2

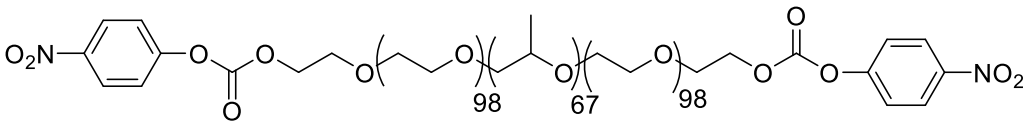

Pluronic® F127 (5 g, 0.40 mmol, 1.00 eq.) was dried at 100^{0}C for 2h and dissolved in 15 mL of dry dichloromethane. 4-nitrophenyl chloroformate (640 mg, 3.18 mmol, 7.95 eq.) was dissolved in 5 mL of dry dichloromethane and slowly added. Finally, pyridine (0.4 mL, 4.96 mmol, 12.50 eq.) was added dropwise, forming a white precipitate. The reaction mixture was stirred at room temperature under Ar atmosphere overnight. The crude was dissolved in 100 mL of dichloromethane and it was washed twice with 150 mL of $NaHSO_4$ 1M and with 150 mL of brine. The organic phase was dried over $MgSO_4$ and concentrated at reduced pressure. The product was precipitated in 300 mL of cold diethyl ether and stored in the refrigerator overnight, filtered and washed with cold diethyl ether to obtain a white powder. Yield: 78%. Mass: 3.91 g.

^{1}H-RMN (400 MHz, $CDCl_3$) δ (ppm): 1.10-1.14 (m, 201 H), 3.33-3.70 (m, ~1100H), 3.78-3.82 (m, 8H), 4-40-4.44 (m, 4H), 7.38 (d, *J*=9.2 Hz, 4H), 8.27 (d, *J*=9.2 Hz, 4H).

FT-IR (neat on NaCl, cm^{-1}): 2864 (ν C-H), 1770 (ν C=O carbonate), 1454 (δ C-H), 1100 (ν C-O-C).

·Synthesis of F127-C-2

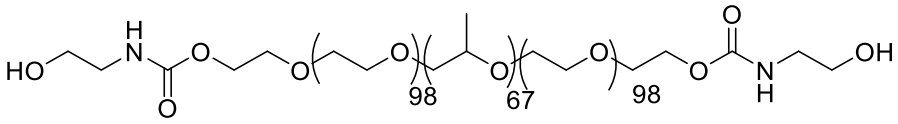

F127-NP-2 (4.26 g, 0.34 mmol, 1.00 eq.) was dried at 100^{0}C for 2h and dissolved in 15 mL dry dichloromethane. Ethanolamine (80 mg, 1.31 mmol, 3.85 eq.) was solved in 10 mL and slowly added, turning the solution yellow. The reaction mixture was stirred at room temperature under Ar atmosphere overnight. The product is precipitated in 200

mL of cold diethyl ether, stored in the refrigerator overnight, filtered and washed with cold diethyl ether to obtain a white powder. Yield: 78%. Mass: 3.30 g.

^{1}H-RMN (400 MHz, $CDCl_3$) δ (ppm): 1.11-1.15 (m, 201 H), 3.30-3.82 (m, ~1100H), 4.20-4.25 (m, 4H), 5.42-5.60 (bs, 2H).

FT-IR (neat on NaCl, cm^{-1}): 3670-3250 (ν O-H), 2870 (ν C-H), 1722 (ν C=O), 1454 (δ C-H), 1107 (ν C-O-C).

·Synthesis of F127-A-2

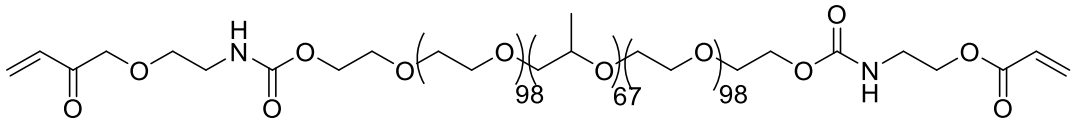

F127-C-2 (1g, 0.079 mmol, 1.00 eq.) was dried at 150^{0}C with vacuum and dissolved in 8 mL of dry dichloromethane. 4-methoxyphenol (130 mg) was added. Triethylamine (0.115 mL, 0.83 mmol, 10.50 eq.) was slowly added and the reaction mixture was cooled down at 0^{0}C and protected from light. After 15 minutes, acryloyl chloride (0.06 mL, 0.74 mmol, 9.40 eq.) was very slowly added, and the reaction mixture was stirred under Ar atmosphere for 48h. The crude is passed through a neutral alumina column, it was precipitated in 10 mL of cold diethyl ether, stored in the refrigerator overnight, filtered and washed with cold diethyl ether to obtain a white powder. Yield: 49%. Mass: 485 mg.

^{1}H-RMN (400 MHz, $CDCl_3$) δ (ppm): 1.11-1.14 (m, 201 H), 3.32-3.82 (m, ~1100H), 4.19-4.25 (m, 8H), 5.12-5.21 (bs, 2H), 5.86 (dd, J_{cis}=10.4 Hz, J_{gem}= 1.4 Hz, 2H), 6.11 (dd, J_{trans}=17.2 Hz, J_{cis}= 10.4 Hz, 2H), 6.42 (dd, J_{trans}=17.2 Hz, J_{gem}= 1.4 Hz, 2H).

FT-IR (neat on NaCl, cm^{-1}): 2882 (ν C-H), 1722 (ν C=O), 1467 (δ C-H), 1107 (ν C-O-C).

4.2. Synthesis of the hybrid dendritic-linear-dendritic Pluronic derivative

·Synthesis of Benzylidene-2,2-bis(oxymethyl)propionic acid

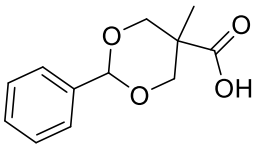

2,2-Bis(hydroxymethyl)-propionic acid (20 g, 149 mmol, 1.00 eq.), benzaldehyde dimethyl acetal (33.6 mL, 224 mmol, 1.50 eq.) and *p*-toluenesulfonic acid monohydrate (1.42 g, 7.45 mmol, 0.05 eq.) were dissolved in 150 mL of dry acetone. The reaction mixture was stirred at room temperature under Ar atmosphere for 4h and then it was stored in the refrigerator overnight. The precipitate was filtered and washed with cold acetone to obtain a white powder. Yield: 59%. Mass: 19.55 g.

^{1}H-RMN (400 MHz, $CDCl_3$) δ (ppm): 1.11 (s, 3H), 3.70 (d, *J*=11.6 Hz, 2H), 4.64 (d, *J*=11.6 Hz, 2H), 5.49 (s, 1H), 7.33-7.38 (m, 3H), 7.45-7.50 (m, 2H).

^{13}C-RMN (100 MHz, $CDCl_3$): δ (ppm): 17.7, 42.2, 73.4, 101.9, 126.1, 128.3, 129.1, 137.5, 178.8.

FT-IR (ATR, cm^{-1}): 3005 (ν OH), 2875 (ν C-H), 1696 (ν C=O).

·Synthesis of Benzylidene-2,2-bis(oxymethyl)propionic anhydride

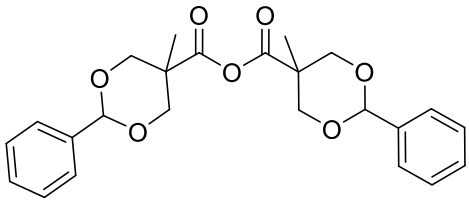

Benzylidene-2,2-bis(oxymethyl)propionic acid (6 g, 27 mmol, 1.00 eq.) was dissolved in 80 mL of dry dichloromethane. N,N´-Dicyclohexylcarbodiimide (3.06 g, 14.85 mmol, 0.55 eq.) dissolved in 10 mL of dry dichloromethane was slowly added. The reaction mixture was stirred at room temperature under Ar atmosphere overnight. A white precipitate appeared and it was filtered off and washed with a small amount of dichloromethane. The organic phase was concentrated at reduced pressure and the product was precipitated into 700 mL of cold hexane. The precipitate was stored at the

refrigerator overnight and it was filtered and washed with cold hexane to obtain a white powder. Yield: 95%.

^{1}H-RMN (400 MHz, $CDCl_3$) δ (ppm): 1.12 (s, 6H), 3.69 (d, *J*=11.6 Hz, 4H), 4.66 (d, *J*=11.6 Hz, 4H), 5.47 (s, 2H), 7.31-7.35 (m, 6H), 7.43-7.48 (m, 4H).

^{13}C-RMN (100 MHz, $CDCl_3$): δ (ppm): 16.8, 44.2, 73.2, 102.1, 126.3, 128.2, 129.3, 137.6, 169.1.

FT-IR (ATR, cm^{-1}): 2875 (ν C-H), 1816 (ν C=O symmetric), 1746 (ν C=O asymmetric).

·Synthesis of F127-Bn-2

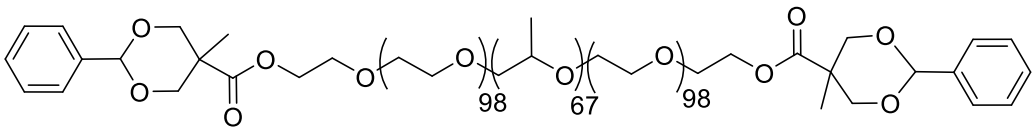

Pluronic® F127 (10 g, 0.79 mmol, 1.00 eq.) was dried at 100^{0}C for 2h and dissolved in 20 mL of dry dichloromethane. 4-Dimethylaminopyridine (320 mg, 2.54 mmol, 3.22 eq.) and 2,2-bis(oxymethyl)propionic anhydride (2.71 g, 6.35 mmol, 8.00 eq.) were added and the reaction mixture was stirred at room temperature under Ar atmosphere overnight. 4 mL of methanol were added and the reaction mixture was stirred for 6h in order to quench the reaction. Then, it was precipitated in 1 L of cold diethyl ether and stored in the refrigerator overnight, filtered and washed with cold diethyl ether to obtain a white powder. Yield: 92%. Mass: 9.45 g.

^{1}H-RMN (400 MHz, $CDCl_3$) δ (ppm): 1.03 (s, 6H), 1.10-1.14 (m, 201H), 3.37-3.80 (m, ~1100H), 4.34 (t, *J*=6.0 Hz, 4H), 4.66 (d, *J*=11.6 Hz, 4H), 5.43 (s, 2H), 7.29-7.33 (m, 6H), 7.39-7.44 (m, 4H).

FT-IR (neat on NaCl, cm^{-1}): 2882 (ν C-H), 1742 (ν C=O, ester), 1107 (ν O-C-O).

·Synthesis of F127-OH-4

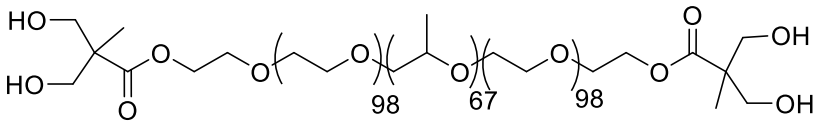

F127-Bn-2 (6 g, 0.48 mmol, 1.00 eq.) was dried at 100^{0}C for 2h and dissolved in 150 mL of ethyl acetate and three vacuum-argon cycles were made. Pd/C (300 mg, 10% (w/w)) was added and another three vacuum-argon cycles were made. Finally, three vacuum-hydrogen cycles were made and the reaction mixture was stirred at room temperature under hydrogen atmosphere overnight. Pd/C was filtered with Celite® and the filtrate was evaporated to obtain a white powder. Yield: 95%. Mass: 5.68 mg.

^{1}H-RMN (400 MHz, $CDCl_3$) δ (ppm): 1.11 (s, 6H), 1.11-1.15 (m, 201 H), 3.34-3.75 (m, ~1100H), 4.31-4.34 (m, 4H).

FT-IR (neat on NaCl, cm^{-1}): 3750-3400 (ν O-H), 2877 (ν C-H), 1739 (ν C=O), 1466 (δ C-H), 1107 (ν C-O-C).

·Synthesis of F127-NP-4

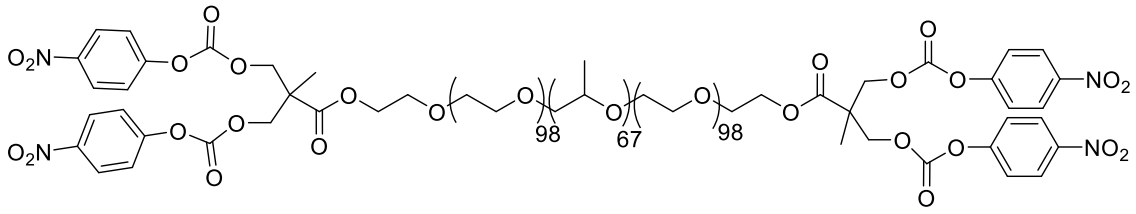

F127-OH-4 (2.3 g, 0.18 mmol, 1.00 eq.) was dried at 100^{0}C for 2h and dissolved in 20 mL of dry dichloromethane. 4-nitrophenyl chloroformate (600 mg, 2.98 mmol, 16.2 eq.) was dissolved in 5 mL of dry dichloromethane and slowly added. Finally, pyridine (0.805 mL, 9.98 mmol, 32.81 eq.) was added dropwise, forming a white precipitate. The reaction mixture was stirred at room temperature under Ar atmosphere overnight. The crude was dissolved in 40 mL of dichloromethane and it was washed twice with 30 mL of $NaHSO_4$ 1M and with 30 mL of brine. The organic phase was dried over $MgSO_4$ and concentrated at reduced pressure. The product was precipitated in 300 mL of cold diethyl ether and stored in the refrigerator overnight, filtered and washed with cold diethyl ether to obtain a white powder. Yield: 78%. Mass: 1.80 g.

^{1}H-RMN (400 MHz, $CDCl_3$) δ (ppm): 1.06-1.21 (m, 201H), 1.38 (s, 6H), 3.32-3.80 (m, ~1100H), 4.34 (t, *J*=4.4 Hz, 4H), 4.46 (d, *J*=10.8 Hz, 4H), 4.57 (d, *J*=11.2 Hz, 4H), 7.36 (d, *J*=9.2 Hz, 8H), 8.25 (d, *J*=8.8 Hz, 8H).

FT-IR (neat on NaCl, cm^{-1}): 2881 (ν C-H), 1770 (ν C=O carbonate), 1465 (δ C-H).

·Synthesis of F127-C-4

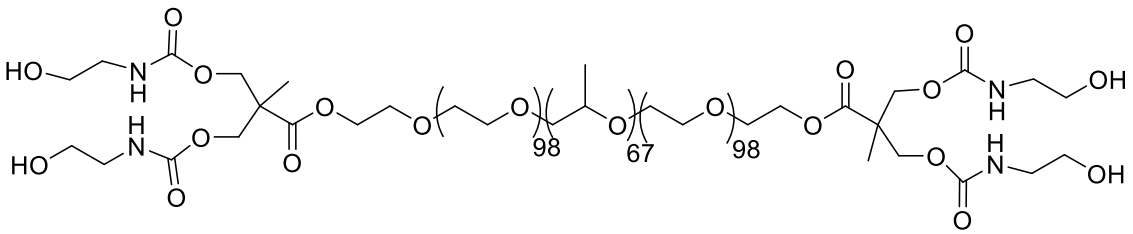

F127-NP-4 (1.75g, 0.13 mmol, 1.00 eq.) was dried at 100^{0}C for 2h and dissolved in 12 mL dry dichloromethane. Ethanolamine (47 mg, 0.77 mmol, 5.92 eq.) was solved in 3 mL of dry dichlorometane and slowly added, turning the solution yellow. The reaction mixture was stirred at room temperature under Ar atmosphere overnight. The product was precipitated in 150 mL of cold diethyl ether, stored in the refrigerator overnight, filtered and washed with cold diethyl ether to obtain a white powder. Yield: 72%. Mass: 1.26 g.

^{1}H-RMN (400 MHz, $CDCl_3$) δ (ppm): 1.06-1.17 (m, 201H), 1.22 (s, 6H), 3.24-3.31 (m, 8H), 3.36-3.81 (m, ~1100H), 4.16-4.31 (m, 12H), 5.62-5.77 (bs, 4H)

FT-IR (neat on NaCl, cm^{-1}): 3594-3220 (ν O-H), 2874 (ν C-H), 1726 (ν C=O), 1465 (δ C-H).

·Synthesis of F127-A-4

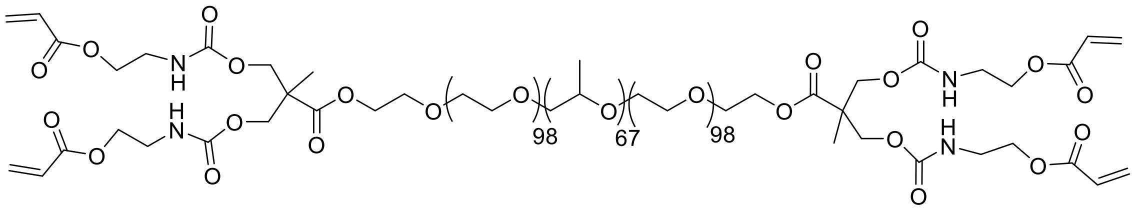

F127-C-4 (1.20 g, 0.091 mmol, 1.00 eq.) was dried at 160^{0}C with vacuum and dissolved in 10 mL of dry dichloromethane. 4-methoxyphenol (250 mg) was added. Triethylamine (0.162 g, 1.60 mmol, 17.60 eq.) was slowly added and the reaction mixture was cooled down at 0^{0}C and protected from light. After 15 minutes, acryloyl chloride (0.132 g, 1.46 mmol, 16.00eq.) was very slowly added, and the reaction mixture was stirred under Ar atmosphere for 48h. The crude is passed through a neutral alumina column, it was precipitated in 10 mL of cold diethyl ether, stored in the refrigerator overnight, filtered and washed with cold diethyl ether to obtain a white powder.

The ^{1}H-NMR spectrum of the partially functionalized compound is depicted in the Annexes.

4.3. Critical Micelle Concentration determination

Solutions of 1.00% (w/v), 0.50% (w/v), 0.30% (w/v), 0.10% (w/v), 0.05% (w/v), 0.01% (w/v), 0.001% (w/v) and 0.0001% (w/v) of the block copolymer in distilled water were prepared in order to carry out the CMC determination. Solutions from 1% (w/v) to 0.1% (w/v) were obtained by direct dissolution of the material in distilled water, whereas solutions from 0.05% (w/v) to 0.0001% (w/v) were obtained by dilution from solutions of higher concentration. All the solutions were kept at 4°C for 4h.

A 1.2·10^{-5} M pyrene solution was prepared by dissolving 0.485 mg of pyrene in 200 mL of distilled water. Due to the low solubility of pyrene in water, it was previously dissolved in 2 mL of acetone and added to 200 mL of distilled water. Finally, acetone was removed at reduced pressure for 4 hours.

10 µL of the pyrene solution were added to the block copolymer solutions, so that the final pyrene concentration within the water solutions was $6 \cdot 10^{-8}$ M. The solutions were incubated at 25°C and protected from light for one hour.

The fluorescence spectra of the solutions were recorded from 300 to 350 nm and $\lambda_{emission}$=390 nm. In order to study the self-aggregation of the materials, intensities at λ=332 nm and λ=335 nm for all the solutions were measured. A representation of the intensities ratio versus the block copolymer concentration was depicted to determine the CMC.

4.4. Photopolymerization of self-assembled micelles

A 10% (w/v) solution of the block copolymer was prepared by dissolving the solid block copolymer in distilled water containing 0.10% (w/v) of the commercial photoinitiator Irgacure 2959. This solution was kept overnight at 4^0C in order to ensure a complete and homogeneous dissolution of the material.

The solution was filtered through a 0.2 µm filter of cellulose acetate to remove suspended particles.

From this 10% (w/v) solution, solutions of 1.4% (w/v), 0.77% (w/v) and 0.50% (w/v) were prepared by diluting with an aqueous solution containing 0.1% (w/v) of Irgacure 2959 previously filtered.

These solutions were kept at room temperature for 1h to reach the equilibrium.

5 mL of these block copolymer solutions were placed in a cylindrical 5 cm diameter glass vessel and photopolymerized by irradiating with UV light (λ=365 nm) for 10 minutes with 8 cm distance between the glass vessel and the lamp. The photopolymerization was carried out at 25^0C. The temperature was controlled by means of a hotplate, on which the glass vessel was placed.

The photopolymerized solutions were dialyzed against distilled water at 4^0C for 24h using a cellulose acetate membrane Spectra/Por® Biotech MWCO 300,000 (Spectrum) with a pore size of 30 nm. The dialysis was carried out to purify the CLPM by removing the unreacted remaining molecules of the block copolymer.

Finally, the dialyzed solutions were filtered again with a 0.2 µm cellulose acetate filter to remove aggregates of sizes bigger than 200 nm.

4.5. Encapsulation of Camptothecin

1mg/mL CPT solution in DMSO was prepared from commercial solid CPT.

Solutions of **F127-A-2-077** and **F127-A-2-140** at 1 mg/mL were prepared by diluting the CLPMs solutions obtained after the polymerization process.

To 2 mL of these solutions, 700 µL of DMSO and 300 µL of CPT 1 mg/mL in DMSO were added, so that the final solution presents a V_{DMSO}:V_{H2O} ratio of 0.5 and a m_{CPT}:$m_{F127\text{-}A\text{-}2}$ ratio of 0.15. Then, these solutions were incubated at room temperature for 24 hours.

DMSO was eliminated by dialysis (Spectra/Por MWCO 2000, Spectrum) for 3 days.

Dialyzed samples were filtered through 0.45 µm PVDF filters in order to eliminate non-encapsulated CPT.

Encapsulated CPT quantification was directly carried out by taking 100 µL the filtered solutions, lyophilizing them and re-dissolving them in a known DMSO volume. Then, CPT was quantified by fluorescence emission spectrum (λ_{max}=436 nm in DMSO with λ_{exc}=368 nm) by using a calibration curve in the concentration range from 11.2 to 39.2 µg/mL in DMSO.

4.6. Encapsulation of Chloroquine

Solutions of **F127-A-2-077** and **F127-A-2-140** at 0.75 mg/mL were prepared by diluting the CLPMs solutions obtained after the polymerization process.

1.33 mL of these solutions were added to 2 mL of dichloromethane and the mixture was incubated for 15 minutes in order to extract the CLPMs from the aqueous phase and dissolve them in the CH_2Cl_2.

A 1.30 mg/mL CQ solution was prepared by dissolving commercial solid chloroquine diphosphate in distilled water.

0.77 mL of the CQ solution were added to the water/CH_2Cl_2 solution containing the CLPMs. Then, in order to remove the CH_2Cl_2, the new mixtures containing both the CLPMs and the drug were mechanically stirred at room temperature until only the aqueous phase was observed, so that the final aqueous solution presented a CLPM and drug concentration of 0.5 mg/mL.

These solutions were dialyzed (Slide-A-Lyzes® Dialysis Cassette G2 2000 MWCO, Thermo Scientific) for 16 hours in order to remove the non-encapsulated drug.

Encapsulated CQ quantification was indirectly carried out by taking samples from the dialysis waters. Non-encapsulated CQ was determined by measuring the absorbance at λ=345 nm and using a calibration curve in the concentration range from 2.5 to 25 µg/mL in distilled water. Encapsulated CQ was then calculated by subtracting the CQ amount present in the dialysis waters to the initial amount of CQ placed in the CLPM containing solution.

5. CONCLUSIONS

The work carried out in this Final Master Project has allowed the following conclusions:

- The chemical modification of Pluronic® F127 with carbamate-based moieties to introduce terminal photopolymerizable acrylate group has enabled the preparation of Cross-Linked Polymeric Micelles, CLPMs.
- The CLPMs present morphologies and sizes, thermosensitive properties, drug load capacities and cell viabilities that make them good candidates for their application as nanocarriers in drug delivery.

6. REFERENCES

[1] A. Bernkop-Schnürch, *European Journal of Pharmaceutical Sciences* **2013**, *50*, 2-7.
[2] S. Stolnik, L. Illum, S. S. Davis, *Advanced Drug Delivery Reviews* **1995**, *16*, 195-214.
[3] F. Masood, *Materials Science and Engineering: C*.
[4] Y. Li, D. Maciel, J. Rodrigues, X. Shi, H. Tomás, *Chemical Reviews* **2015**, *115*, 8564-8608.

[5] K. Yoncheva, P. Calleja, M. Agüeros, P. Petrov, I. Miladinova, C. Tsvetanov, J. M. Irache, *International Journal of Pharmaceutics* **2012**, *436*, 258-264.
[6] M. W. Grinstaff, *Journal of Polymer Science Part A: Polymer Chemistry* **2008**, *46*, 383-400.
[7] W. I. Choi, G. Tae, Y. H. Kim, *Journal of Materials Chemistry* **2008**, *18*, 2769-2774.
[8] A. Gulzar, S. Gai, P. Yang, C. Li, M. B. Ansari, J. Lin, *Journal of Materials Chemistry B* **2015**, *3*, 8599-8622.
[9] R. Pelton, *Advances in Colloid and Interface Science* **2000**, *85*, 1-33.
[10] R. Basak, R. Bandyopadhyay, *Langmuir* **2013**, *29*, 4350-4356.
[11] D. A. Chiappetta, A. Sosnik, *European Journal of Pharmaceutics and Biopharmaceutics* **2007**, *66*, 303-317.
[12] G. Whitton, E. R. Gillies, *Journal of Polymer Science Part A: Polymer Chemistry* **2015**, *53*, 148-172.
[13] N. Feliu, M. V. Walter, M. I. Montañez, A. Kunzmann, A. Hult, A. Nyström, M. Malkoch, B. Fadeel, *Biomaterials* **2012**, *33*, 1970-1981.
[14] I. Jiménez-Pardo, R. González-Pastor, A. Lancelot, R. Claveria-Gimeno, A. Velázquez-Campoy, O. Abian, M. B. Ros, T. Sierra, *Macromolecular Bioscience* **2015**, *15*, 1381-1391.
[15] I. Jimenez-Pardo, Doctoral Thesis thesis, University of Zaragoza **2014**.
[16] H. Ihre, O. L. Padilla De Jesús, J. M. J. Fréchet, *Journal of the American Chemical Society* **2001**, *123*, 5908-5917.
[17] M. Ashjari, S. Khoee, A. Mahdavian, R. Rahmatolahzadeh, *J Mater Sci: Mater Med* **2012**, *23*, 943-953.
[18] C. Khemtong, C. W. Kessinger, J. Gao, *Chemical Communications* **2009**, 3497-3510.
[19] X. Li, Q. Wu, Z. Chen, X. Gong, X. Lin, *Polymer* **2008**, *49*, 4769-4775.
[20] C. Pinto Reis, R. J. Neufeld, A. J. Ribeiro, F. Veiga, *Nanomedicine: Nanotechnology, Biology and Medicine* **2006**, *2*, 8-21.
[21] J. Movellan, P. Urbán, E. Moles, J. M. de la Fuente, T. Sierra, J. L. Serrano, X. Fernàndez-Busquets, *Biomaterials* **2014**, *35*, 7940-7950.
[22] P. Agrawal, U. Gupta, N. K. Jain, *Biomaterials* **2007**, *28*, 3349-3359.
[23] P. Melnyk, V. Vingtdeux, S. Burlet, S. Eddarkaoui, M.-E. Grosjean, P.-E. Larchanché, G. Hochart, C. Sergheraert, C. Estrella, M. Barrier, V. Poix, P. Plancq, C. Lannoo, M. Hamdane, A. Delacourte, P. Verwaerde, L. Buée, N. Sergeant, *ACS Chemical Neuroscience* **2015**, *6*, 559-569.
[24] L. Fan, M. Degen, N. Grupido, S. Bendle, P. Pennartz, *Materials Science and Engineering: A* **2010**, *528*, 127-136.
[25] aK. J. Blight, J. A. McKeating, C. M. Rice, *Journal of Virology* **2002**, *76*, 13001-13014; bV. Lohmann, F. Körner, J.-O. Koch, U. Herian, L. Theilmann, R. Bartenschlager, *Science* **1999**, *285*, 110-113; cS. Susser, J. Vermehren, N. Forestier, M. W. Welker, N. Grigorian, C. Füller, D. Perner, S. Zeuzem, C. Sarrazin, *Journal of Clinical Virology* **2011**, *52*, 321-327; dA. Urbani, R. Bazzo, M. C. Nardi, D. O. Cicero, R. De Francesco, C. Steinkühler, G. Barbato, *Journal of Biological Chemistry* **1998**, *273*, 18760-18769.